A multi-criteria support system for UAV maritime surveillance in a highly dynamic environment

Kyriacos Antoniades[a], Alessio Ishizaka[b], Jana Ries[c]
Portsmouth Business School
Centre of Operational Research and Logistics
University of Portsmouth
PO3 1ED, Portsmouth, UK

Abstract - The aim of this paper is to implement a maritime surveillance decision support system for navigating unmanned aerial vehicles (UAVs) to investigate a set of maritime vehicles (MVs) in an area of interest (AOI). As the sea environment is highly uncertain and dynamic, it requires the routing calculation to be highly responsive to changes and to operate online. The online adaptive routing system integrates the two multi criteria decision analysis (MCDA) methodologies AHP and PROMETHEE, a geographical information system (GIS) and a mathematical programming (MP) method. The order of the MV investigation is based on their degree of *suspiciousness*. This system provides a first step toward intelligent autonomous UAVs. To demonstrate the functionality of this decision support system, a combined drug trafficking and illegal immigration surveillance case study is presented.

Keywords – OR in Defence, Dynamic Unmanned Air Vehicle Routing, AHP, PROMETHEE, GIS

1 Introduction

Unmanned Aerial Vehicles are deployed when the presence of on board human pilots is too risky. Their lower operational cost (as compared to manned aircraft and satellites) and their availability to be customized in a large variety of sizes and capabilities makes them even more attractive for maritime surveillance (Hanscom & Bedford; Lowe, Story, & Parsons, 2014; Teo, 2013; Wargo, Church, Glaneueski, & Strout, 2014). However, UAVs are often not completely autonomous as they are piloted remotely from the Ground Control Station (GCS) following the indications of a human operator. The aim of this study is to increase further the autonomy of UAVs by developing an online decision support system that will automate a

[a] Kyriacos.Antoniades@port.ac.uk
[b] Alessio.Ishizaka@port.ac.uk
[c] Jana.Ries@port.ac.uk

UAV's navigation path for maritime surveillance; on the basis of *suspiciousness* for a set of maritime vehicles in an area of interest. The aim of each UAV is thus, to achieve effective and efficient maritime surveillance in an environment that is continuously changing: new MVs appear (or disappear), their speed and heading changes, their *environmental factors* may vary, etc. The goal of the proposed decision support system is to indicate to a UAV at any instance of time, which MV out of the set is the most *suspicious* and therefore of high priority to be investigated immediately. To solve this problem, four methods have been used in combination. These include:

1. AHP (Analytic Hierarchy Process)
2. PROMETHEE (Preference Ranking Organization METhod for Enrichment Evaluation)
3. MP (Mathematical Programming)
4. GIS (Geographical Information System)

The ranking of suspicious MVs can be deemed as a multi-criteria problem, because several **environmental factors** *sub criteria* related to the MVs can serve as determinants to evaluate their suspiciousness. Consequently, the weight given to each environmental *sub criterion* also depends on the **mission** *criteria* that the UAV has to undertake. To obtain the overall *criteria weights (suspiciousness)*, a criteria hierarchy has been constructed (Section 4.2) and calculated with AHP (Section 4.3, Section 4.4). This activity can be planned as an a priori scenario and recorded for further a posteriori utilisation. The overall *criteria weights* are then reported to all UAVs having PROMETHEE independently installed, which rank at every instance of time a set of simultaneously targeted MVs (Section 4.5) based on their *suspiciousness*. Thereafter, the geographical information system (GIS) utilizing the above mentioned ranking data together with the automatic identification system's (AIS) data availability of real time locations of all UAVs and MVs; it records per time interval, the current location of each UAV together with calculated location of the target (most *suspicious*) MV in the next interval of time to allow to calculate the new heading (route) for this UAV in real time. This, also allows for the customization of the GIS system to provide for the overall view (visualization) of the running scenario of operation and further performance analysis of the mission (Section 4.6) after it has been completed. Finally, in case of two or more UAVs rank equally an MV to investigate immediately, a mathematical programming method can be used to break the tie by uniquely assigning a UAV to a specific MV, by maximising the PROMETHEE net flows (Section 4.7).

Details of the above mentioned methodologies are discussed further in the succeeding sections. The structure of the paper is as follows. Section 2 discusses how multi-criteria decision analysis (MCDA) methods have been used in the defence sector. Section 3 describes the proposed solution combining the four methods as described above. Section 4 illustrates a case study, followed by the conclusions in Section 5.

2 Literature review

Decisions in the defence sector often need to consider a large number of factors of conflicting nature. Therefore, multi-criteria decision analysis methods have been extensively used. It has permitted to increase the operational efficiency in several areas (Aull–Hyde & Davis, 2012).

For example, they have been used in ***resource allocation***. Gass (1986), has combined goal programming and AHP for planning the personnel in the US Army over a seven-year horizon. Partovi and Epperly (1999), have combined the Quality Function Deployment and AHP to determine the composition of a United States peacekeeping force deployed to Bosnia. Korkmaz, Gökçen, and Çetinyokus (2008), have used AHP to match open positions in US navy and personal preferences of military personnel. Bigham, Cuthbert, Yang, Lu, and Ryan (2004), use AHP for selecting a telecommunication network and upgrading or downgrading existing connection. They also utilise a weighted sum to allocate bandwidth in telecommunications networks. Trainor, et al. (2007), have used an additive value model to find the best number of US Army installation regions. They discovered that four regions were the best number to manage. Crary, Nozick, and Whitaker (2002), combined AHP, mixed integer programming and simulation to find the most effective mix of cruisers, guided missile destroyers and new destroyers. AHP and multiple-objective optimisation was used to allocate Finnish Defence Forces to 12 Military Provinces (Haapalinna, 2003) and a limited number of aircraft for missions (Stannard, Zahir, & Rosenbloom, 2006).

Multi-criteria decision methods have been used in ***performance analysis***. Seven US generals, representing the greatest wartime commander, were ranked with AHP (Retchless, Golden, & Wasil, 2007). Rough-AHP combined with TOPSIS have been used to measure performance of aviation firms (Aydogan, 2011). Fuzzy sets are applied for performance appraisal and ranking of candidates in military organisations (Moon, Lee, & Lim, 2010).

Several applications cover ***weapons selection and evaluation***. AHP has been used to evaluate Korean ground weapon systems (Y. Lee & Ahn, 1991) and GPS systems for the Israeli Defence Force (Israeli, Mehrez, Bochen, & Hakim, 1998). AHP has later been combined with Fuzzy logic (Cheng & Mon, 1994) to select and anti-aircraft artillery and to select attack helicopters (Cheng, Yang, & Hwang, 1999), with Fuzzy Topsis to select infantry rifle (Dagdeviren, Yavuz, & KilInç, 2009), and with principal component and goal programming for selecting surface-to-air missile systems (J. Lee, Kang, Rosenberger, & Kim, 2010). Greiner, Fowler, Shunk, Carlyle, and McNutt (2003), use AHP followed by an integer programming for screening weapon systems development projects to be accomplished within a constrained resource environment. Fuzzy sets were used to select tactical missile systems (Chen, 1996) and battle tanks (Cheng & Lin, 2002).

MCDA has been applied to ***strategic and operational planning***. In 1980, AHP has been used to decide if 53 American hostages from Teheran should have been rescued or not (TL Saaty, Vargas, & Barzilay, 1982). It has been also applied in an action selection by Great Britain after the Falklands Islands invasion in a post-analysis (TL Saaty, 1983). Fuzzy ANP followed by Fuzzy TOPSIS and Fuzzy ELECTRE have been applied to select a sniper (Kabak, Burmaoğlu, & Kazançoğlu, 2012).

Another application includes ***risk analysis***. Merrick and Harrald (2007), use multi-attribute utility theory to analyse the safety in US ports and waterways. Finan and Hurley (2002), use AHP for evaluating the threats and their probability against Canada's national interests.

From this literature review, it can be seen that MCDA methods have received much attention in defence due to their simplicity, ease of use and justifiability. Recently, there has been an increase of hybrid methods utilization. Single methods seem insufficient to provide an effective and realistic analysis of complex situations due to its inherent assumptions.

The presented case is very complex due to the dynamic behaviour of the scenario. Therefore, as explained in the next section, a multiple method solution has been adopted to implement UAV autonomy.

3 Methodology

3.1 General overview

We consider a set K of n suspect Maritime Vehicles MV_k and a set S of m Unmanned Airborne Vehicles UAV_j. The suspiciousness p_k of each MV_k is evaluated on n criteria c_i. As the criteria may depend on the initial location of the UAV_j, the urgency of the intervention on an MV_k is different for each UAV_j and therefore, the priority ranking of the MV_k will be different for each UAV_j. Furthermore, the ranking will change after each single intervention as the environment is highly dynamic and thus a sequential and iterative decision making process is adopted. Figure 1 shows a schematic overview of the decision support system, including the methods used, their data exchanges and interfaces.

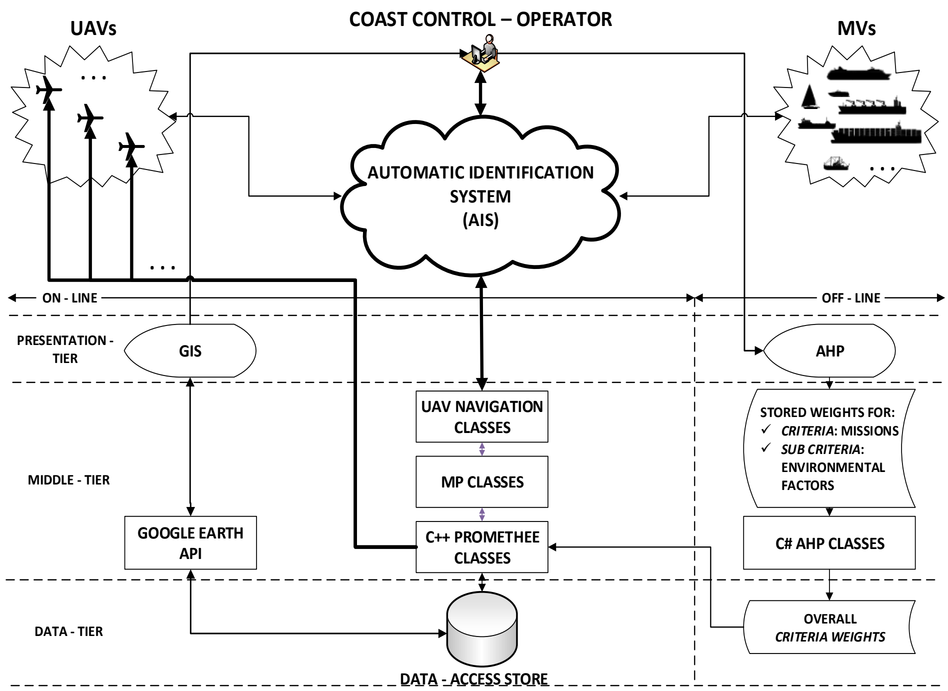

Figure 1: General overview of the decision support system (arrows indicate data flow)

The application is planned to be integrated with the automatic identification system as used by operators in the coast ground control (CGC). It is developed on a three-tier architecture, splitting the application functionality into three logical units of tiers. This encourages reusability, easy documentation and structured analysis. In addition, it allows the overall system to be resistant to changes, as when one tier is either improved or altered, the other tiers remain unaffected. The presentation-tier contains the graphical user interface (GUI) and includes the functions that manage the interaction between the operator and the middle-tier.

The middle-tier receives requests from the presentation-tier and returns results back to the presentation-tier according to the processing algorithms it contains. The middle-tier also calls the data-tier for information. The data-tier is responsible for storing the application data and sending it to the middle-tier as required. It is noted that the AHP methodology is an off-line process, meaning that all criteria weights calculations are predetermined. PROMETHEE, MP and GIS are online processes. The stages of the developed decision support system in relation to each of the methods and their respective input(s) and output(s) are briefly summarized in Table 1. The next sections describe all four stages in more detail.

Table 1: Processing stages of the developed decision support system at a particular decision making sequence in time; arrows indicate data flow.

METHOD	STAGE	INPUT	EXECUTION	OUTPUT
AHP	Pre-processing (offline)	A-priory expert pairwise comparisons of UAV mission criteria and MV environmental factors sub criteria	Weights calculations	Overall Criteria Weights (stored in database)
PROMETHEE		Weights of environmental factors criteria that determine *suspiciousness* MV data	Priority calculations	Ranking of suspicious MVs (stored in database)
MP	Processing (online)		Checks if two of more UAVs are allocated the same MV	**FALSE** Continue with original allocation (stored in database) **TRUE** Uniquely assign a UAV to a specific MV (stored in database)
GIS		***Real time*** locations of all sets of UAVs and MVs provided by **AIS**	Google Earth	Visualization of UAVs and MVs
	Post-processing (offline)	UAV_j to MV_k assignment		A-posteriori route path analysis

3.2 AHP: Strategic definition and weighting of suspiciousness criteria

The first stage focuses on structuring the problem with the definition of the UAV mission criteria and MV environmental factors sub criteria, as used to measure the suspiciousness of MVs. In this exercise, it is necessary to elicit the acquired knowledge of experienced human UAV operators. Once the problem is structured, the pairwise comparison of the importance of each criterion is evaluated in a comparison matrix A. Weights are calculated with Saaty's (1977) eigenvalue method of AHP:

$$A \cdot p = \lambda_{max} \cdot p \qquad (1)$$

where, A is the comparison matrix

p is the priority (weight) vector

λ_{max} is the maximal eigenvalue

A consistency of the evaluations can be measured with the consistency index (CI):

$$\mathrm{CI} = \frac{\lambda_{max} - n}{n - 1} \qquad (2)$$

where, *n* is the dimension of the matrix

λ_{max} is the maximal eigenvalue

If the consistency ratio of the consistency and the random indexes is less than 10%, then the matrix can be considered as having an acceptable consistency (A Ishizaka & Labib, 2011; T Saaty, 1980).

3.3 PROMETHEE: Ranking of suspicious maritime vehicles

In the second stage, the suspiciousness of the maritime vehicles is ranked using PROMETHEE. It has been adopted mainly because once its parameters are defined, it can be fully automated. It also has a very low computing time, which is essential in a dynamic environment for online manipulations. Moreover, the particular method does not require technical parameters and therefore it can be easily explained and be used by non-technical personnel (Alessio Ishizaka & Nemery, 2013). A normalisation of the scores in not needed and therefore the evaluation of each criterion can be expressed in its own units. By consequence, it avoids the drawback of the ranking being dependent on the selected normalisation method. PROMETHEE compares pairwise the suspiciousness of each maritime vehicle, by calculating the difference between the suspiciousness criteria evaluation of the two MVs on the criterion *i*:

$$d_i(MV_k, MV_f) = f_i(MV_k) - f_i(MV_f) \tag{3}$$

where, $d_i(MV_k, MV_f)$ is the difference between the evaluations of two alternatives (i.e. MVs) for one criterion f_i.

This difference is introduced in the preference function of criterion *i*, which gives the unicriterion preference degree. Several preference functions exists (Brans & Vincke, 1985), e.g. the linear (4), the step or Gaussian (5) preference function.

$$P_{kf}^{i} = \begin{cases} 0, & if\ d_i(MV_k, MV_f) \leq q_i \\ \dfrac{d_i(MV_k, MV_f) - q_i}{p_i - q_i}, & if\ q_i < d_i(MV_k, MV_f) \leq p_i \\ 1, & if\ d_i(MV_k, MV_f) > p_i \end{cases} \tag{4}$$

where, q_i is the indifference threshold

p_i is the preference threshold

$$P_{kf}^{i} = \begin{cases} 1 - exp\left(\dfrac{-\left(d_i(MV_k, MV_f)\right)^2}{2{s_i}^2}\right), & if \quad d_i(MV_k, MV_f) \geq 0 \\ 0, & otherwise \end{cases} \tag{5}$$

where, s_i is the inflection point.

The global preference degree is given by the weighted sum of the unicriterion preference degree:

$$\pi(MV_k, MV_f) = \sum_{i=1}^{n} P_{kf}^{i}(MV_k, MV_f) \cdot w_i \tag{6}$$

where, w_i represents the weight of criterion c_i

In order to compare every maritime vehicle with respect to all the others, two scores are computed. The positive outranking flow (7) expresses how a maritime vehicle outranks all the others. It represents its power (outranking) character. The higher $\phi^+(MV_k)$ is, the more preferred the action is. The negative outranking flow (8) expresses how a maritime vehicle is outranked by all the others. It is its weakness, its outranked character. The lower $\phi^-(MV_k)$ is, the worse the action is.

$$\phi^+(MV_k) = \frac{1}{n-1} \sum_{MV \in K} \pi(MV_k, MV) \tag{7}$$

$$\phi^-(MV_k) = \frac{1}{n-1} \sum_{MV \in K} \pi(MV, MV_k) \tag{8}$$

Thence, the positive and negative preference flows are aggregated into the net preference flow:

$$\phi(MV_k) = \phi^+(MV_k) - \phi^-(MV_k) \tag{9}$$

The PROMETHEE ranking is obtained by ordering the alternatives (MVs) according to the decreasing values of the net flow scores.

3.4 UAV Navigation

Each MV and UAV is tabulated in a file, based on the guidelines of the Earth Point site (Clark, 2015). Then, each file is converted to a Keyhole Mark-up Language (KML) file, using the Earth Point tools provided. This allows to simulate the sequential MV allocation problem so as to utilize Google Earth as a visualization tool.

In every instance and for each MV_k, the AIS provides their initial geographic coordinates $(lat_{MV_\kappa}(t), lon_{MV_\kappa}(t))$ in radians, as well as their initial bearing in degrees, $BRG_{MV_K}(t)$, at time, t (i.e. *initial time*). Based on this information, the location of each MV_k, $(lat_{MV_\kappa}(t'), lon_{MV_\kappa}(t'))$ and bearing travelling along a (shortest distance) great circle arc $BRG_{MV_K}(t')$ for the next time instance t' (i.e. *final time*), are calculated. Thence, once the rankings of MVs suspiciousness scores are obtained, a UAV is instructed to change its direction (route) and lock to the MV with the highest ranking (i.e. being most suspicious). In other words, we wish to navigate an UAV at time t, to the location of the most suspicious MV with coordinates $(lat_{MV_\kappa}(t'),\ lon_{MV_\kappa}(t'))$. At time, t_0 = *0*, for each UAV (as shown in Figure 2) their position can be defined by $(lat_{UAV}(t_0), lon_{UAV}(t_0))$ which is the initial starting point (latitude, longitude) of the UAV in radians and $BRG_{UAV}(t_0)$ which is the initial bearing of the UAV in radians, clockwise from North. The destination point of the UAV, $(lat_{UAV}(t), lon_{UAV}(t))$ and final predicted heading travelling along a (shortest distance) great circle arc $(HDG_{UAV}(t))$ in the next time interval, t, towards the most suspicious MV, is calculated using the Movable Type Scripts (Veness, 2014):

$$lat_{UAV}(t) = \operatorname{asin}(\sin(lat_{UAV}(t_0)) \times \cos\left(\frac{d}{ER}\right) + \cos(lat_{UAV}(t_0)) \times \sin\left(\frac{d}{ER}\right) \times \cos(BRG_{UAV}(t_0)) \quad (\text{:}$$

where, d is the distance travelled by a UAV per time interval

ER is the Earth's Radius (6371 km) d / ER is the angular distance (radians)

$$lon_{UAV}(t) = lon_{UAV}(t_0) + atan2(w, x) \quad (11)$$

where,

$$w = \cos\left(\frac{d}{ER}\right) - \sin(lat_{UAV}(t)) \times \sin(lat_{UAV}(t_0)) \quad (12)$$

$$x = \sin(BRG_{UAV}(t_0)) \times \sin\left(\frac{d}{ER}\right) \times \cos(lat_{UAV}(t_0)) \quad (13)$$

The new UAV heading is calculated by:

$$HDG_{UAV}(t) = atan2(y, z) \quad (14)$$

where,

$$y = \cos(lat_{UAV}(t)) \times \sin(lat_{MV_\kappa}(t)) - \sin(lat_{UAV}(t)) \times \cos(lat_{MV_\kappa}(t)) \times \cos(lon_{MV_\kappa}(t) - lon_{UAV}(t)) \quad (\text{:}$$

$$z = \sin(lon_{MV_\kappa}(t) - lon_{UAV}(t)) \times \cos(lat_{MV_\kappa}(t)) \quad (\text{:}$$

Thereafter, the process is repeated for each interval of time to route the UAV to the most suspicious MV.

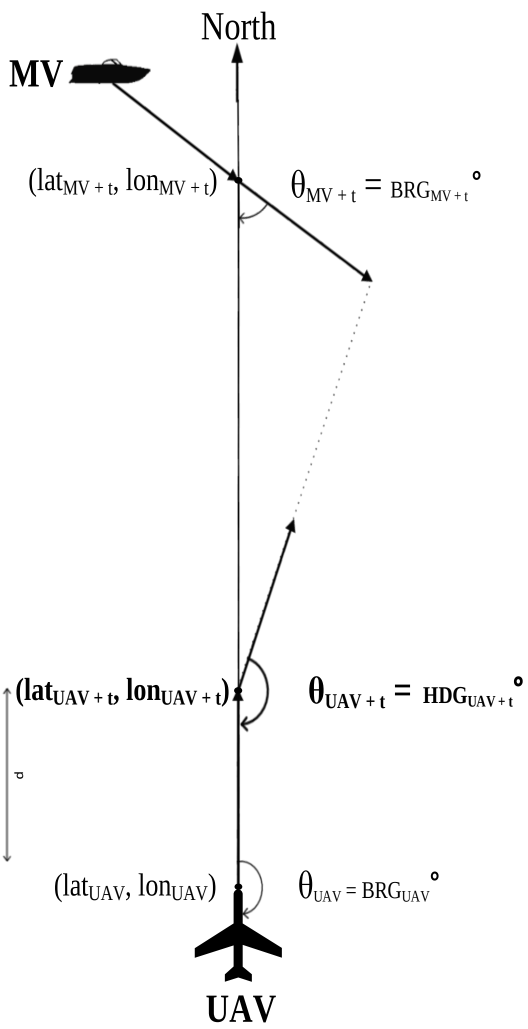

Figure 2 UAV navigation

Finally, the distance of the UAV to the most suspicious MV, $Dist_{UAV-MV}$ is determined (to allow making the decision when to terminate the investigation) by the spherical laws of cosines (at sea level):

$$Dist_{UAV-MV} =$$

$$\mathrm{acos}(\sin(lat_{UAV}(t)) \times sin(lat_{MV_K}(t)) + \cos \times lat_{UAV}(t) \times \cos(lat_{MV_K}(t)) \times \cos(lon_{MV_K}(t) - lon_{UAV}(t))) \times ER \quad (\text{:}$$

Considering that the UAV is flying at a certain height, *h*, from the sea level, we thus use Pythagoras's theorem of equirectangular projection, to calculate the actual distance, D_A of the UAV_j to the most suspicious MV_k (Figure 3).

$$D_A = \sqrt{Dist_{UAV-MV_\kappa}{}^2 + h^2} \tag{18}$$

As an assumption, the UAVs will stay locked to the MV until the distance between them is less than or equal to the maximum camera range, which is the maximum range that a UAV can investigate (i.e. photograph) the suspicious MV.

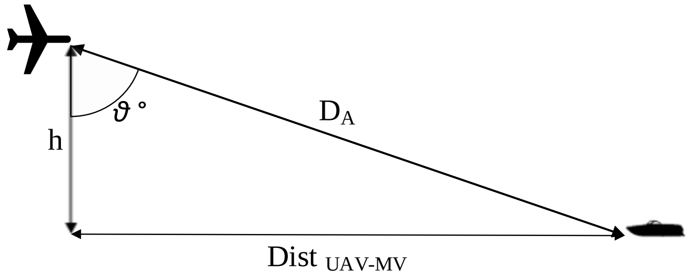

Figure 3 Actual distance

If this condition is satisfied (UAV completes the investigation of the MV), then the specific MV is removed from the list of UAVs to investigate and a new PROMETHEE ranking is re-calculated to define the next MV to investigate. This procedure is repeated, until all MVs are investigated.

3.5 GIS: Visualization

A Geographic Information System (GIS) allows to visualize, question, analyse, and interpret data on a geographical map to understand relationships, patterns, and trends (Lidouh, 2013; Lidouh, Smet, & Zimányi, 2011; Malczewski, 1999). GIS allows the collection of data which can be overlain on the base map to create geo-referenced renderings. It is a tool that links features on a maps with data. The linking of map features and data is commonly known as 'spatial data' and it proved to be useful when integrated with AHP and PROMETHEE methodologies (Alemu, 2011; Feizizadeh, Jankowski, & Blaschke, 2013; Joerin, Thériault, & Musy, 2001; Nasiri, et al., 2013; Xu & Zhang, 2013). It allows to create distinct map layers for each UAV and MV, and then by overlaying on Google Earth to visualize the whole scenario collectively in real time. Each layer consists of spatial data describing the route path of each MV and the calculated routing path of each UAV. As this information is stored in the database, the GIS module implemented should improve a posteriori decision-making by enabling supplementary analysis of the data.

3.6 MP: Multiple UAV allocation

In case of two or more UAVs having the same first allocated target, the tie is broken by modelling an assignment problem (19). The global objective function is to maximise the total suspiciousness of the MVs that will be investigated by the fleet of UAVs. If UAV_j is sent to observe MV_k, then x_{jk} is assigned 1 otherwise 0.

$$max \sum_{j \in S} \sum_{k \in K} p_{jk} \cdot x_{jk} \tag{19}$$

subject to:

$$\forall k \in K \ \sum_{j=1}^{m} x_{jk} = 1 \ [for\ each\ \ MV_k\ at\ most\ one\ UAV_j\ is\ allocated]$$

$$\forall j \in S \ \ \sum_{k=1}^{n} x_{jk} = 1 \ [for\ each\ UAV_j\ at\ most\ one\ MV_k\ is\ assigned]$$

$$x_{jk} \in (0,1), \quad \forall j \in S, \quad \forall k \in K$$

where, p_{jk} is the suspiciousness value calculated by PROMETHEE.

After a MV has been fully investigated, it is removed from the list of suspect MVs, while the criteria characteristics of the remaining (unvisited) MVs are updated. PROMETHEE is used again to calculate a ranking for the next assignment (see section 3.3).

4 Case Study

4.1 Introduction

In order to test the aforementioned methodology, a case study with 15 MVs is illustrated. Figure 4 shows their initial location and their arrow indicates their direction. MV_1, MV_2, MV_3 and MV_4 are considered suspicious in the context of drug trafficking. Specifically, MV_1, MV_2,

MV_3 are small speed boats initially starting from the shores of Sicily. They all meet with MV_4, a large cargo ship travelling parallel to the shore of Sicily and approximately 70 kilometres from the coast; which also detours slightly inwards to the coast to meet with the speed boats. The speed boats meet the cargo ship consecutively. After a so-called rendez-vous (agreed meeting location), all speed boats return to the shores of Sicily and the cargo ship resumes original bearing as before detouring (Figure 11). The remaining marine vehicles $MV_5 – MV_{15}$ are considered suspicious for illegal immigration.

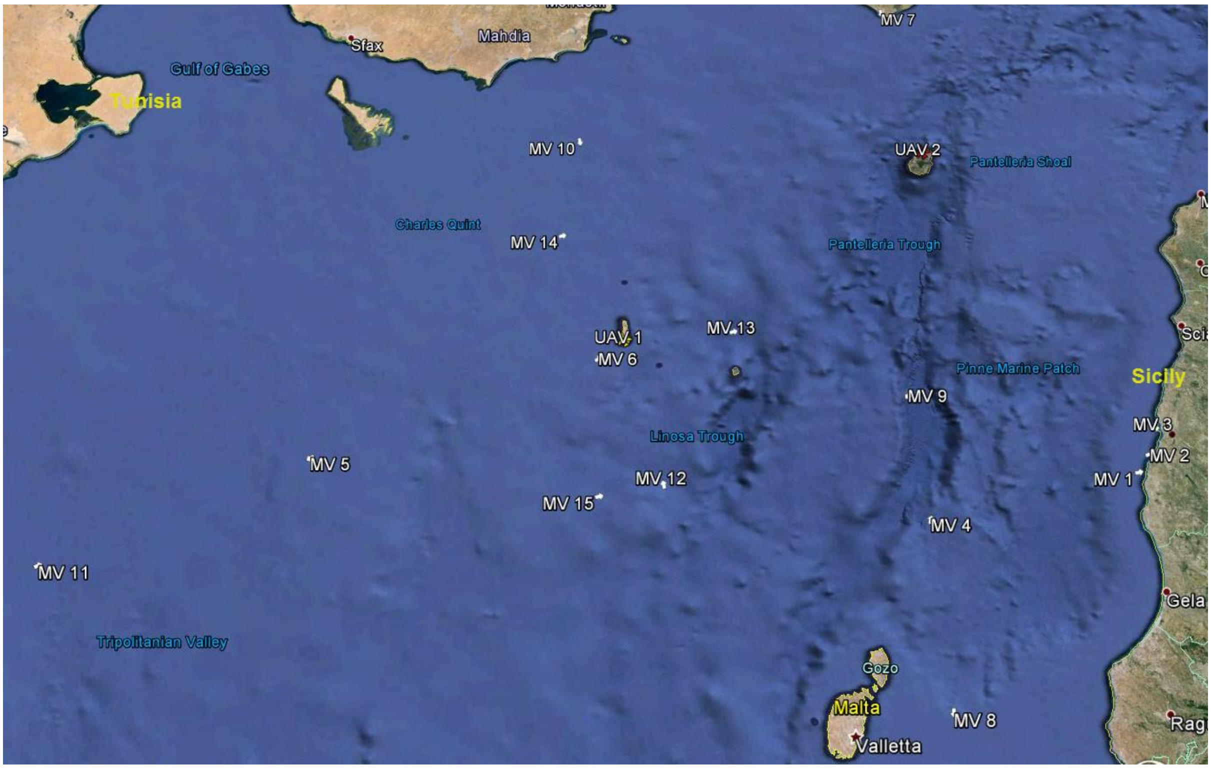

Figure 4: Google Earth simulation for 2 UAVs and 15 MVs at initial time: 16:30

Two UAVs are chosen to implement the surveillance of the fifteen suspicious MVs. UAV_1 taking off from Lampedusa and UAV_2 taking off from Pantelleria. Figure 4 shows the locations of the two UAVs and the 15 MVs at initial time 16:30. The simulation is run in intervals of 5 minutes, until 20:20. In the next section, UAV mission criteria and MV environmental sub criteria are determined.

4.2 AHP: Hierarchy Design

In a brainstorming exercise with seven sea boarder surveillance experts, a list of UAV mission criteria and MV environmental sub criteria have been elicited. Four mission criteria have been considered for the theatre of the operations. These include:

a) Drug trafficking near the island (Lampedusa)
b) Drug trafficking near the coast (Marina di Palma)
c) Illegal immigration during the day
d) Illegal immigration during the night

The missions are evolving and not mutually exclusive. For example, drug trafficking and illegal immigration can happen at the same time. For each UAV mission, the definition of *suspiciousness* is determined by the MV environmental sub criteria, which are the same for each mission criteria, but their importance (weights) are different. These include:

C_1: *Dimension of the MV* [m]: smaller MVs are more suspicious, especially if they are traveling fast and they become more difficult to detect.

C_2: *Change of speed* [km/h]: large increases or decreases of MV's speed for no particular reason increases suspiciousness. For example, a decrease in the speed of MVs could mean that they could be slowing down to approach each other, whereas sudden increase of the speed of small MVs makes them ultimately more suspicious for both drug trafficking or illegal immigration.

C_3: *Rendez-vous* [km]: A small distance between MVs could indicate a meeting, probably to exchange illicit goods. The distance between the MV and its closest neighbour is recorded.

C_4: *Distance to island* [km]: The closest of the island (e.g. Lampedusa in mission a), the more urgent an investigation is, which may indicate illegal immigration.

C_5: *Distance to coast* [km]: The closest to the coast (e.g. Marina di Palma in mission b), the more urgent an investigation is, which may indicate drug trafficking.

C_6: *Distance UAV to MV* [km]: The shorter the 'travel time' will be. Hence, the faster a UAV can reach at the MV of interest.

C_7: *MAOC tagging* [binary criterion (0 = false; 1 = true)]: the operator in Maritime Analysis and Operations Centre (MAOC) has information to indicate that the MV is highly suspicious and recommend an urgent investigation.

The distances *Being close to island* (C4) and *Being close to coast* (C5) are further processed with the Area Criteria Algorithm (ACA) to define the urgency (A.1). These criteria have and output values between 0 and 1, where 1 indicates an extreme urgency and 0 means that it is not urgent. The Change of speed (C_2), Distance to island (C_4), Distance to coast (C_5), and the MAOC tagging (C_7) criteria are to be maximized in PROMETHEE. The remaining criteria are to be minimised. In the Appendix, it can be seen how the criteria are calculated. The structure (scenario) of the problem (Figure 5) has two levels, where the suspiciousness of the maritime vehicles, will depend on the defined UAV missions' *criteria* and the environmental factors *sub criteria* pertaining to each MV.

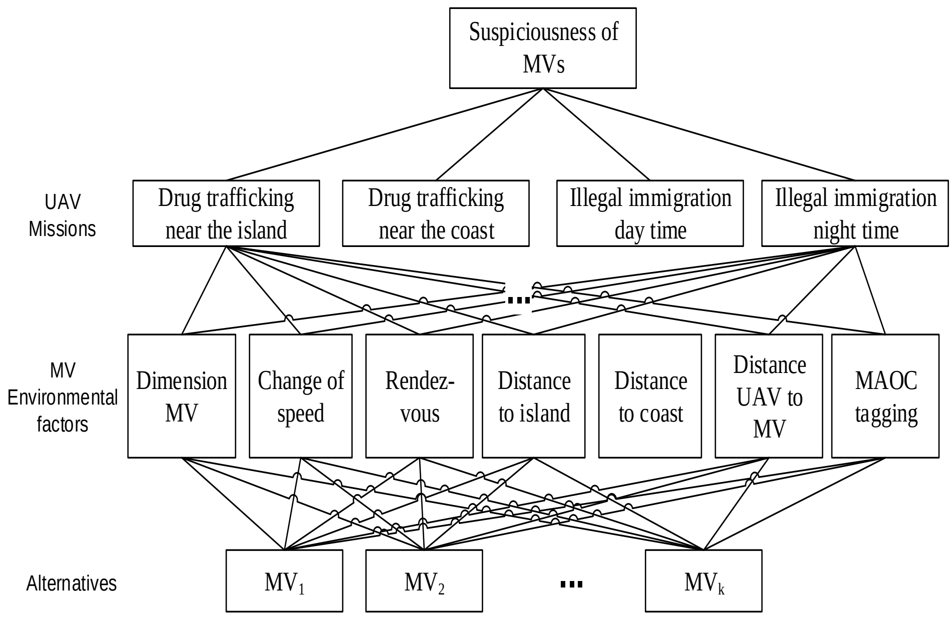

Figure 5: Hierarchy - defining the criteria and sub criteria

4.3 AHP: Mission criteria weighting

Although the mission starts for both UAV_1 and UAV_2 simultaneously, due to their different geographical location, the scenario is thus different for each UAV. UAV_1 is more concerned with illegal immigration, whilst UAV_2 is more dedicated to drug trafficking. By consequence, their scenario weights are different. The most appropriate scenario is evaluated by the experts using pairwise comparisons in Figure 6 for UAV_1 and in Figure 7 for UAV_2. A customised AHP software has been developed in C#, where the graphical interface is shown in Figure 6 and Figure 7. The scenario priorities are given in Table 2.

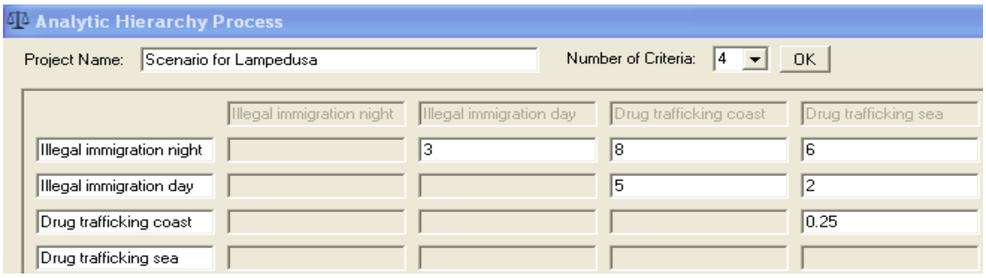

Figure 6: Pairwise comparisons of the scenario for UAV_1

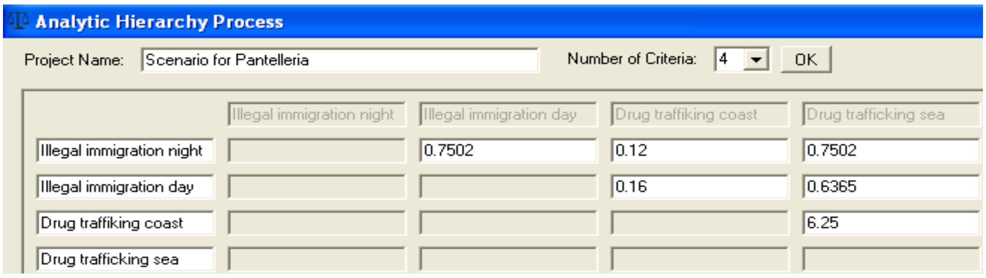

Figure 7: Pairwise comparisons of the scenario for UAV_2

Table 2: Mission priorities for each UAV scenarios

	Priorities	
	***UAV*₁** UAV_1	UAV_2
Drug trafficking near the island	0.1307	0.1249
Drug trafficking near the coast	0.0488	0.6925
Illegal immigration during the day	0.2259	0.0995
Illegal immigration during the night	0.5946	0.0831
Consistency ratio	0.043	0.0001

4.4 AHP: Environmental criteria weighting

The criteria defined in section 4.2, are prioritised using pairwise comparisons by the sea border surveillance experts for all missions (Figure 8). The calculated weights are given in Table 3.

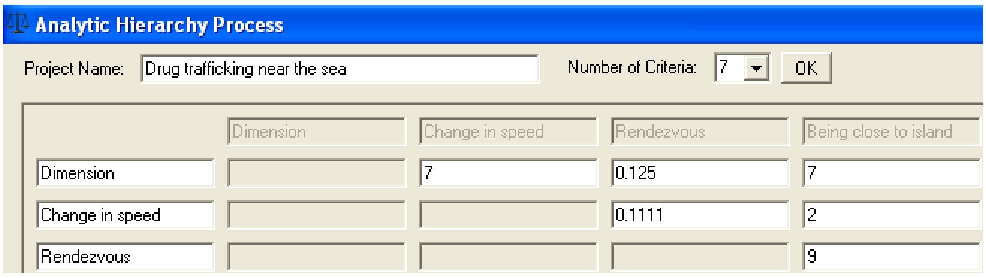

Figure 8: Pairwise comparison of the environmental criteria for the drug trafficking near the coast mission

Table 3: Weight of the environmental criteria for the drug trafficking near the coast mission

Criteria	**Weight**
Dimension	0.1708
Change in speed	0.0394
Rendez-vous	0.0402
Distance to island	0.0337
Distance to coast	0.3194
Distance UAV to MV	0.0337
MAOC tagging	0.4258
Consistency Ratio (CR)	0.0571

Table 4 gives the weights for all the missions. All comparison matrices are consistent (i.e. CR ≤ 10 %). The MAOC tagging is the most weighted criterion. This result was expected as the MAOC is based on the possession of external information (operator opinion) indicating a particularly high suspicious MV. In our case study all MVs are tagged. The distance to coast is highly important in the scenario ’Drug trafficking near the coast‘. In the other scenarios the coast may be far away and therefore this criterion is less important. As a rendez-vous in the middle of the sea is highly improbable because MVs tend not to be close to each other in order to avoid collisions, this behaviour is highly suspicious. A change of speed in the night is unlikely because of security reasons. Therefore it has a higher weight in the night scenario. The distance UAV to MV obtains generally a low weight because UAVs are much faster than MVs.

Table 4: Environmental criteria weights for different mission criteria

Criteria	Drug coast	Drug sea	Immigration	Immigration
Dimension	0.171	0.103	0.092	0.165
Change of Speed	0.039	0.023	0.031	0.144
Rendez-vous	0.040	0.321	0.025	0.020
Distance to island	0.034	0.020	0.155	0.063
Distance to coast	0.319	0.033	0.150	0.221
Distance UAV to MV	0.034	0.166	0.030	0.083
MAOC tagging	0.426	0.334	0.518	0.304
Consistency Ratio (CR)	0.06	0.09	0.07	0.09

As the UAVs are operating with different mission criteria (section 4.3). Their criteria weights for each UAV is shown in Table 5.

Table 5: The final suspiciousness criteria weights for each UAV

	Criteria	UAV_1	UAV_2
C_1	Dimension	0.139	0.111
C_2	Change of Speed	0.104	0.047
C_3	Rendez-vous	0.052	0.079
C_4	Distance to island	0.069	0.044
C_5	Distance to coast	0.184	0.252
C_6	Distance UAV to MV	0.084	0.059
C_7	MAOC tagging	0.358	0.408

The criteria weights for UAV_1 and UAV_2 are used to dynamically rank MVs using PROMETHEE as is described in the next section.

4.5 PROMETHEE: Dynamic MV ranking

Fifteen MVs are to be investigated. For each MV, their location, heading and speed are transmitted to the decision support system by the automated identification system or if absent by fixed land radars and satellites. The sub criteria *dimension* (C_1) is independent of time and the considered UAV. *Change of speed* (C_2), *rendez-vous* (C_3), *distance to island* (C_4), *distance to coast* (C_5) and to some extent the *MAOC* (C_7) tagging are time-dependent but independent from the observing UAV. The *Distance UAV to MV* (C_6) is dependent on time and the observing UAV. Table 6 presents an extract of time-dependent sub-criteria scores.

Table 6: Extract of time-dependent scores for MV_1 with regards to UAV_1

				C_2	**C_3**	**C_4**	**C_5**	**C_6**
Time	**lat_{MV}** (degrees)	**lon_{MV}** (degrees)	**HDG** (degrees)	**Change of speed** (ms^{-1})	**Rendez-vous** (km)	**Distance to island** (km)	**Distance to coast** (km)	**Distance UAV_1 to MV_1** (km)
16:30	37.1461	13.7059	200.63	0.0000	9.0425	0.6915	0.6849	207.0257
16:35	37.1461	13.7059	200.63	0.0000	9.0425	0.6915	0.6849	219.7014
16:40	37.1461	13.7059	200.63	0.0000	9.0425	0.6915	0.6849	214.0965
16:45	37.1461	13.7059	200.63	0.0000	9.0425	0.6915	0.6849	197.4209
16:50	37.1461	13.7059	200.63	0.0000	9.0425	0.6915	0.6849	206.0995
16:55	37.1461	13.7059	200.63	0.0000	7.5013	0.6915	0.6849	213.4439
17:00	37.1461	13.7059	200.63	0.0000	8.5816	0.6915	0.6849	193.9330
17:05	37.1461	13.7059	200.63	0.0000	11.5778	0.6915	0.6849	173.9472
17:10	37.1071	13.6875	200.61	0.0000	11.2630	0.6739	0.5405	152.5922
17:15	37.0681	13.6691	200.6	0.0010	10.9650	0.6630	0.5555	127.9802
17:20	37.0291	13.6507	200.59	0.0010	10.6851	0.6588	0.5670	138.1652
17:25	36.9901	13.6324	200.58	0.0094	10.4326	0.6627	0.5768	126.8471
17:30	36.951	13.614	200.57	0.0461	10.1794	0.6756	0.5825	102.2279
17:35	36.912	13.5957	200.56	0.0441	9.9716	0.6983	0.5874	77.6257
17:40	36.873	13.5774	200.55	0.0010	9.7798	0.7310	0.5910	53.1178
17:45	36.834	13.5592	200.54	0.0094	9.6280	0.7732	0.5952	28.5549
17:50	36.795	13.5409	200.53	0.0114	9.4847	0.8219	0.5971	4.5125
17:55	36.756	13.5227	200.52	0.0094	9.3888	0.8742	0.5998	19.1984
18:00	36.7169	13.5045	200.5	0.0357	9.2981	0.9257	0.6011	5.7426
18:05	36.6779	13.4863	200.49	0.0338	4.6832	0.9659	0.6028	9.9207
18:10	36.6389	13.4681	200.48	0.0010	0.5352	0.9898	0.6041	14.7098
18:15	36.6389	13.4681	200.48	0.0000	4.6173	0.9898	0.6041	6.5799

Scores of the first allocation (16:30) for UAV_1 are given in Table 7. Scores of the second allocation (16:50) for UAV_1 are given in Table 8. The weights of the criteria are provided from Table 5.

Table 7: Tables of scores on the first Allocation to UAV_1 at time 16:30

	C_1	C_2	C_3	C_4	C_5	C_6	C_7
Min/Max	**MIN**	**MAX**	**MIN**	**MAX**	**MAX**	**MIN**	**MAX**
Pref. fn	Linear	Linear	Linear	Linear	Linear	Linear	Linear
Preference	20	0.001	20	n/a	n/a	40	1
Indifference	8	0	2	n/a	n/a	10	0
Inflection point	n/a	n/a	n/a	n/a	n/a	n/a	n/a
Weight	***0.139***	***0.104***	***0.062***	***0.069***	***0.184***	***0.084***	***0.358***
MV_1	12	0.00000	9.04250	0.69147	0.68487	207.04077	1
MV_2	8	0.00000	9.04250	0.97286	0.55079	210.29712	1
MV_3	20	0.00000	11.64001	0.98518	0.90812	212.09093	1
MV_4	60	0.00000	46.41567	0.91941	0.84256	135.96395	1
MV_5	12	0.00000	108.86166	0.80510	0.91403	131.73642	1
MV_6	8	0.00000	55.75107	0.70678	0.94084	12.78534	1
MV_7	20	0.00000	151.58211	0.70403	0.57698	201.14370	1
MV_8	60	0.00000	78.06388	0.66111	0.76819	188.33113	1
MV_9	12	0.00000	46.41567	0.67515	0.81765	114.48565	1
MV_{10}	8	0.00000	46.23095	0.97737	0.95039	95.32083	1
MV_{11}	20	0.00000	108.86166	0.97383	0.72887	240.57696	1
MV_{12}	60	0.00000	25.35867	0.95862	0.81954	61.45869	1
MV_{13}	12	0.00000	55.75107	0.72816	0.77170	44.69734	1
MV_{14}	8	0.00000	46.23095	0.66058	0.80624	53.96599	1
MV_{15}	20	0.00000	25.35867	0.67760	0.57915	66.14128	1

The MV ranking (suspiciousness score) calculated by PROMETHEE is given in Figure 9. UAV_1 routes to investigate MV_6 as it is the first ranked.

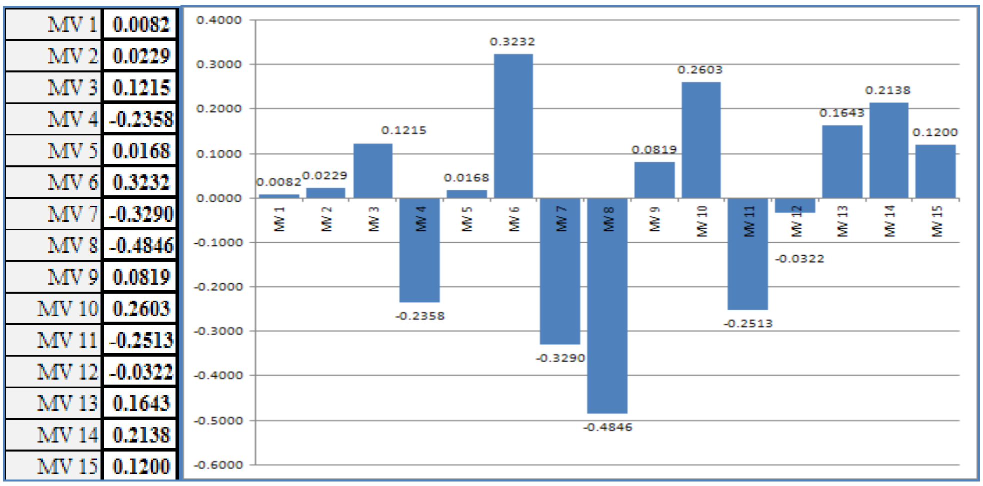

Figure 9. Rankings for the first allocation at time 16:30

Table 8: Tables of scores on the second allocation to UAV_1 at time 16:50

	C1	**C_2**	**C_3**	**C_4**	**C_5**	**C_6**	**C_7**
Min/Max	**MIN**	**MAX**	**MIN**	**MAX**	**MAX**	**MIN**	**MAX**
Pref. fn	Linear	Linear	Linear	Linear	Linear	Linear	Linear
Preference	20	0.001	20	1	1	40	1
Indifference	8	0	2	0	0	10	0
Inflection point	n/a	n/a	n/a	n/a	n/a	n/a	n/a
Weight	***0.139***	***0.104***	***0.062***	***0.069***	***0.184***	***0.084***	***0.358***
MV_1	12	0.00000	9.04250	0.69147	0.68487	197.56713	1
MV_2	8	0.00000	9.04250	0.97286	0.55079	201.40350	1
MV_3	20	0.03698	11.00964	0.97719	0.57768	195.00890	1
MV_4	60	0.04139	30.39690	0.93922	0.65700	122.14995	1
MV_5	12	0.00005	74.32397	0.82517	0.85629	137.18672	1
MV_7	20	0.00000	150.36530	0.89930	0.63807	200.43476	1
MV_8	60	0.00000	86.26048	0.99441	0.65932	167.19565	1
MV_9	12	0.04541	30.39690	0.66304	0.82941	95.35236	1
MV_{10}	8	0.00000	36.62439	0.97492	0.69900	101.88671	1
MV_{11}	20	3.02194	74.32397	0.96626	0.96110	211.03315	1
MV_{12}	60	0.00000	26.62310	0.94939	0.82114	37.29339	1
MV_{13}	12	0.00000	47.85059	0.72816	0.77170	43.97994	1
MV_{14}	8	0.00000	36.62439	0.66058	0.80624	71.30158	1
MV_{15}	20	0.00000	26.62310	0.67760	0.57915	52.57409	1

At 16:50, UAV_1 investigation of MV_6 is completed and thus removed from the PROMETHEE rankings (Table 8). Also, the suspiciousness of remaining MVs have changed (Figure 10).

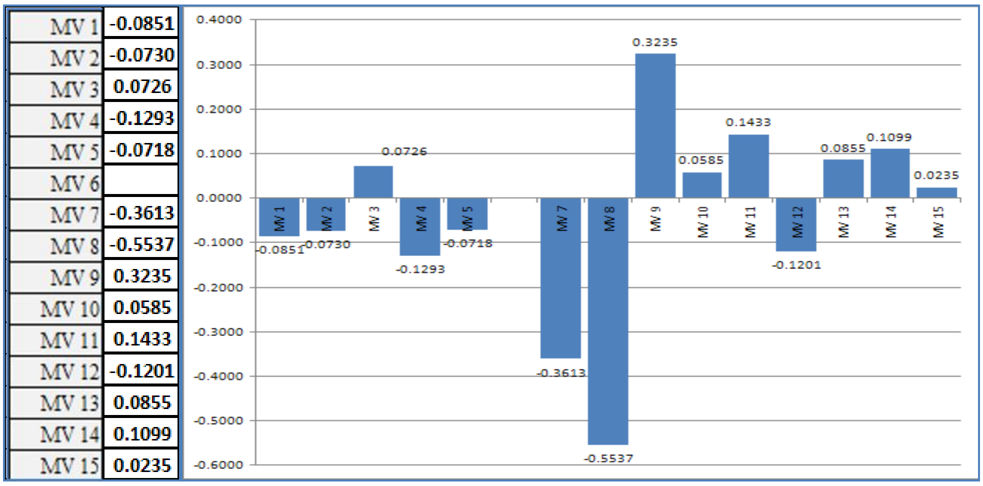

Figure 10. Rankings for the second allocation at time 16:50

The new ranking shows that MV_9 is now most suspicious (e.g. it is now near to the island and its speed has increased) and thus it is the next MV to be investigated. When MV_9 investigation in then completed, the table of scores is updated and a new PROMETHEE ranking is re-calculated. This procedure is also simultaneously repeated for UAV_2 (taking off from Pantelleria). In the next section the final results for UAV_1 and UAV_2 routing visualization on the Google Earth GIS is discussed.

4.6 GIS: Route visualization

Given the initial UAV coordinates and heading (i.e. take-off at the airport) and the coordinates and heading of the most suspicious MV, the sequential MV allocation is calculated with the methodology presented in section 3.4. Table 9 shows an extract of the dynamic routing of UAV_1, the succession of the MVs to investigate and their distances ($Dist_{uav\_mv}$).

Table 9: UAV_1 routing

UAV_1: ILLEGAL IMMIGRATION				**MV to investigate and its coordinates**				
Time	**lat_{uav}**	**lon_{uav}**	**HDG**	**lat_{MV}**	**lon_{MV}**	**HDG_{uav}**	**$Dist_{uav\_mv}$**	**MV#**
16:30	35.4995	12.6273	260.2839	35.3967	12.6842	155.73	12.54	**6**
16:35	35.4689	12.4096	102.7402	35.4208	12.6692	102.74	24.11	**6**
16:40	35.4291	12.6249	58.5916	35.4450	12.6569	58.59	3.40	**6**
16:45	35.5227	12.8135	28.3120	36.2742	13.3164	28.31	95.05	**9**
16:50	35.6810	12.9186	34.2708	36.2189	13.3736	34.27	72.50	**9**
16:55	35.8295	13.0435	43.0567	36.1636	13.4308	43.06	50.93	**9**
17:00	35.9609	13.1952	57.9803	36.1083	13.4878	57.98	31.00	**9**
17:05	36.0561	13.3838	91.2867	36.0531	13.5447	91.29	14.47	**9**
17:10	36.0518	13.6062	183.9150	35.9978	13.6017	183.92	6.03	**9**
17:15	35.8724	13.5911	359.3418	37.0044	13.5748	359.34	125.88	**2**
17:20	36.0522	13.5885	358.6782	36.9640	13.5622	358.68	101.41	**2**
17:25	36.2321	13.5834	357.7696	36.9235	13.5497	357.77	76.94	**2**
17:30	36.4118	13.5747	356.3598	36.8831	13.5372	356.36	52.51	**2**
17:35	36.5913	13.5605	353.5027	36.8426	13.5247	353.50	28.13	**2**
17:40	36.7700	13.5351	330.3907	36.8022	13.5122	330.39	4.12	**2**
17:45	36.9263	13.4239	130.4235	36.8340	13.5592	130.42	15.82	**1**
17:50	36.8096	13.5949	251.3965	36.7950	13.5409	251.40	5.07	**1**
17:55	36.7520	13.3822	213.5312	35.8981	12.6853	213.53	113.64	**13**
18:00	36.6020	13.2584	213.4572	35.8981	12.6853	213.46	93.64	**13**
18:05	36.4519	13.1351	213.3839	35.8981	12.6853	213.38	73.64	**13**
18:10	36.3016	13.0123	213.3110	35.8981	12.6853	213.31	53.64	**13**
18:15	36.1513	12.8900	213.2387	35.8981	12.6853	213.24	33.64	**13**
18:20	36.0008	12.7681	213.1670	35.8981	12.6853	213.17	13.64	**13**
18:25	35.8501	12.6467	33.0958	35.8981	12.6853	33.10	6.36	**13**
18:30	36.0008	12.7681	320.9628	36.8331	11.9219	320.96	119.57	**7**
18:35	36.1404	12.6278	320.8802	36.8331	11.9219	320.88	99.57	**7**
18:40	36.2798	12.4871	320.7970	36.8331	11.9219	320.80	79.57	**7**

18:45	36.4191	12.3458	320.7133	36.8331	11.9219	320.71	59.57	**7**
18:50	36.5583	12.2040	320.6290	36.8331	11.9219	320.63	39.57	**7**
18:55	36.6972	12.0617	320.5441	36.8331	11.9219	320.54	19.57	**7**
19:00	36.8360	11.9189	140.4586	36.8331	11.9219	140.46	0.43	**7**
19:05	36.6972	12.0617	164.5499	34.1319	12.9169	164.55	295.58	**5**
19:10	36.5238	12.1213	164.6532	34.1439	12.9094	164.65	274.12	**5**
19:15	36.3504	12.1804	164.7622	34.1558	12.9019	164.76	252.66	**5**
19:20	36.1768	12.2390	164.7969	34.1558	12.9019	164.80	232.66	**5**
19:25	36.0032	12.2973	164.8312	34.1558	12.9019	164.83	212.66	**5**
19:30	35.8296	12.3553	164.8652	34.1558	12.9019	164.87	192.66	**5**
19:35	35.6560	12.4131	164.8990	34.1558	12.9019	164.90	172.66	**5**
19:40	35.4823	12.4707	164.9325	34.1558	12.9019	164.93	152.66	**5**
19:45	35.3086	12.5280	164.9657	34.1558	12.9019	164.97	132.66	**5**
19:50	35.1349	12.5850	164.9986	34.1558	12.9019	165.00	112.66	**5**
19:55	34.9612	12.6418	165.0312	34.1558	12.9019	165.03	92.66	**5**
20:00	34.7874	12.6984	165.0635	34.1558	12.9019	165.06	72.66	**5**
20:05	34.6136	12.7547	165.0956	34.1558	12.9019	165.10	52.66	**5**
20:10	34.4398	12.8108	165.1274	34.1558	12.9019	165.13	32.66	**5**
20:15	34.2659	12.8667	165.1589	34.1558	12.9019	165.16	12.66	**5**
20:20	34.0920	12.9223	345.1902	34.1558	12.9019	345.19	7.34	**5**

Table 9 shows the complete routing path for UAV_1 and all the MVs. Table 10 shows the complete routing path for UAV_2 and all the MVs. Figure 11 shows the complete routing path for both UAV_1 (yellow path) and UAV_2 (red path) together with all the MVs (white path). All tracking is done using Google Earth GIS as a visualization tool. The full GIS simulation can be seen on http://www.ishizaka-dev.myweb.port.ac.uk/Simulation.mp4.

Table 10*:* UAV_2 routing

UAV$_2$ DRUG TRAFFICKING				**MV to investigate and its coordinates**				
Time	**lat$_{uav}$**	**lon$_{uav}$**	**HDG**	**lat$_{MV}$**	**lon$_{MV}$**	**HDG$_{uav}$**	**Dist$_{uav_mv}$**	**MV#**
16:30	36.8005	11.9557	260.2839	37.2637	13.5275	69.27	148.72	**3**
16:35	36.7699	11.7344	70.4339	37.2637	13.5275	70.43	168.40	**3**
16:40	36.8300	11.9461	72.2138	37.2223	13.5226	72.21	146.59	**3**
16:45	36.8847	12.1602	74.3111	37.1808	13.5177	74.31	124.91	**3**
16:50	36.9332	12.3769	76.8516	37.1393	13.5128	76.85	103.40	**3**
16:55	36.9739	12.5961	80.0652	37.0978	13.5080	80.07	82.10	**3**
17:00	37.0047	12.8180	84.4062	37.0563	13.5031	84.41	61.09	**3**
17:05	37.0220	13.0422	91.0014	37.0148	13.4983	91.00	40.50	**3**
17:10	37.0187	13.2674	104.0458	36.9733	13.4934	104.05	20.69	**3**
17:15	36.9748	13.4858	177.0362	36.9319	13.4886	177.04	4.78	**3**
17:20	36.7952	13.4974	192.3737	34.3381	12.8453	192.37	279.52	**11**
17:25	36.6195	13.4494	193.2500	34.4261	12.8239	193.25	250.38	**11**
17:30	36.4444	13.3982	194.2797	34.5142	12.8025	194.28	221.31	**11**

17:35	36.2701	13.3431	195.5305	34.6022	12.7806	195.53	192.33	**11**
17:40	36.0968	13.2835	197.0658	34.6903	12.7589	197.07	163.47	**11**
17:45	35.9248	13.2184	199.0345	34.7783	12.7372	199.03	134.74	**11**
17:50	35.7548	13.1461	201.7010	34.8664	12.7156	201.70	106.23	**11**
17:55	35.5876	13.0643	205.6358	34.9544	12.6939	205.64	78.02	**11**
18:00	35.4254	12.9688	212.4022	35.0425	12.6722	212.40	50.38	**11**
18:05	35.2735	12.8507	228.9826	35.1306	12.6500	228.98	24.19	**11**
18:10	35.1554	12.6847	323.7919	35.2186	12.6281	323.79	8.72	**11**
18:15	35.3004	12.5546	353.5515	35.5253	12.5233	353.55	25.16	**10**
18:20	35.4791	12.5298	353.5372	35.5253	12.5233	353.54	5.16	**10**
18:25	35.6579	12.5048	232.8116	35.3767	12.0517	232.81	51.57	**14**
18:30	35.5490	12.3287	232.7091	35.3767	12.0517	232.71	31.57	**14**
18:35	35.4399	12.1531	232.6071	35.3767	12.0517	232.61	11.57	**14**
18:40	35.3306	11.9779	52.5057	35.3767	12.0517	52.51	8.43	**14**
18:45	35.4399	12.1531	99.1698	35.2825	13.3061	99.17	106.01	**15**
18:50	35.4111	12.3710	99.2961	35.2825	13.3061	99.30	86.01	**15**
18:55	35.3818	12.5887	99.4222	35.2825	13.3061	99.42	66.01	**15**
19:00	35.3522	12.8062	99.5481	35.2825	13.3061	99.55	46.01	**15**
19:05	35.3221	13.0236	99.6739	35.2825	13.3061	99.67	26.01	**15**
19:10	35.2917	13.2408	99.7994	35.2825	13.3061	99.80	6.01	**15**
19:15	35.2609	13.4579	352.7779	36.5422	13.2558	352.78	143.63	**4**
19:20	35.4393	13.4302	351.7521	36.5403	13.2315	351.75	123.72	**4**
19:25	35.6173	13.3984	350.6596	36.5487	13.2077	350.66	104.97	**4**
19:30	35.7948	13.3624	349.3462	36.5570	13.1839	349.35	86.25	**4**
19:35	35.9716	13.3213	349.3221	36.5570	13.1839	349.32	66.25	**4**
19:40	36.1483	13.2801	344.8244	36.5736	13.1364	344.82	49.01	**4**
19:45	36.3219	13.2216	341.3942	36.5819	13.1126	341.39	30.51	**4**
19:50	36.4923	13.1502	333.2503	36.5902	13.0888	333.25	12.19	**4**
19:55	36.6529	13.0493	166.9834	36.5985	13.0650	166.98	6.21	**4**
20:00	36.4777	13.0997	201.7197	35.5094	12.6264	201.72	115.78	**12**
20:05	36.3105	13.0171	201.4744	35.5094	12.6303	201.47	95.65	**12**
20:10	36.1431	12.9356	194.0485	35.5094	12.7408	194.05	72.62	**12**
20:15	35.9686	12.8816	188.6209	35.5094	12.7961	188.62	51.64	**12**
20:20	35.7908	12.8484	179.5029	35.5094	12.8514	179.50	31.29	**12**

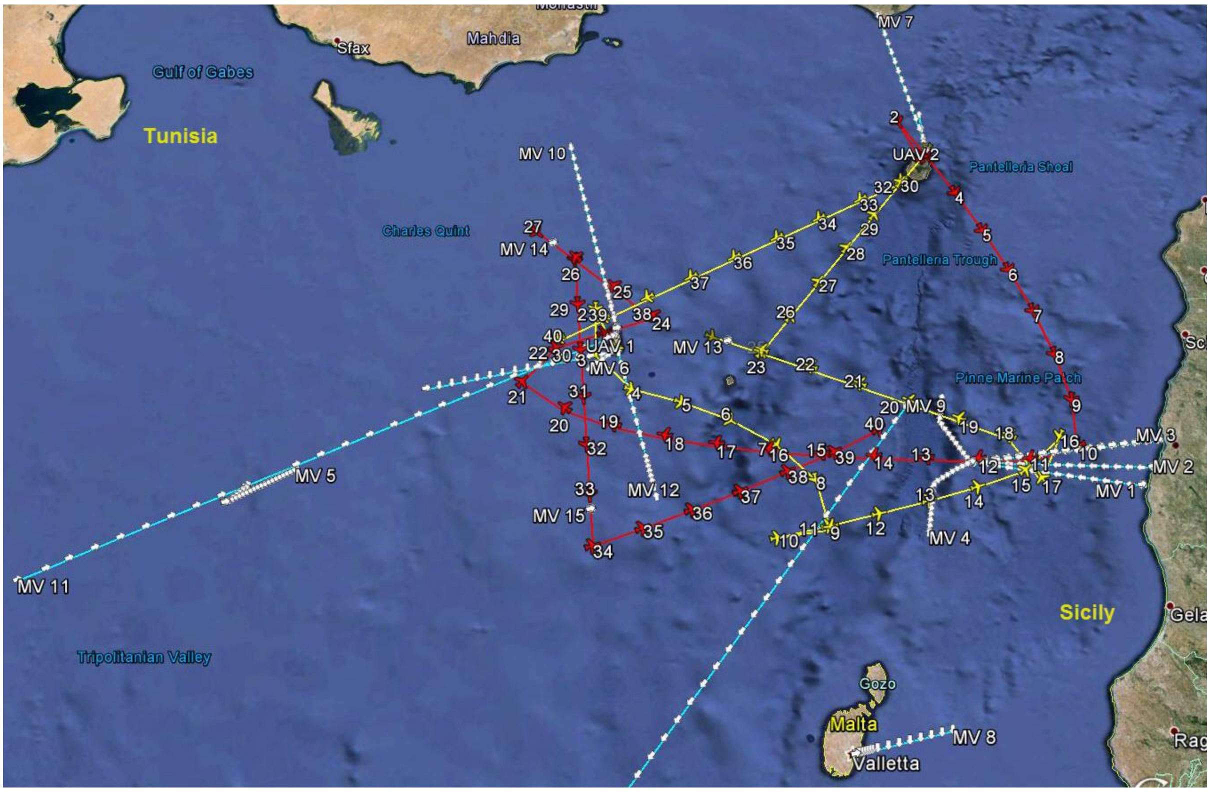

Figure 11: *UAV_1* and *UAV_2* routing

On Table 9 and Table 10, the behaviour of the two UAVs can be analysed. *UAV_1* was operating with more important weight for the illegal immigration mission. *UAV_2* was assigned a higher weight for the drug trafficking mission (Table 2). It can be seen that the order of investigation of the UAVs does not necessarily follow their main mission, for example, *MV_{11}* is the second one investigated by *UAV_2*, which is suspected for illegal immigration. *MV_4*, which is the cargo ship that is under suspicion of transferring drug to a speed boat, is investigated late because it is slow and large, which means that it can be located easily at any point of time. *MV_5* and *MV_{12}* are last investigated because they are located far of the coast, travelling at very low speed (occasionally remain stationary) and showing low variation in velocity.

4.7 MP: Multiple UAV allocation

In this particular case study, there are no ranking ties between any MVs by the two UAVs (Table 10). Nevertheless, it is deemed that as the number of UAVs and MVs increases, the possibility of ranking ties would come into action and the mathematical programming methodology for solving the assignment problem between two MVs with equal rank ties, as presented in section 3.4, would then facilitate in determining the most suspicious MV for each UAV.

5 Conclusion

The sea border is by far the largest and most challenged border of several countries in Europe (e.g. United Kingdom, Italy, Spain, Greece, etc.). For example, the border of the European Union is 70'000 km, twice the length of the Russia border and three times the USA border. The extend of illegal immigration, drug trafficking, contraband and tax fraud has recently increased and creates an unbearable burden especially on small islands (Malta, Mayotte, Canary Islands, Lampedusa, etc.). In addition to the large area of interest, the surveillance is done under highly dynamic conditions: MVs appear and disappear, their speed and heading changes, environmental factors vary, etc. In this paper, we have proposed a decision support system to increase the effectiveness and efficiency of maritime surveillance by means of UAVs. Due to the high complexity and the level of dynamism of the context, a stand-alone method cannot solve the problem. Therefore, an integrated approach combining AHP, PROMETHEE, GIS and mathematical programming techniques has been proposed. The flexibility of these methods permits their integration into a hybrid model. AHP is used to establish the mission and environmental weights. This task is done off-line as it is time intensive and also may require a debate between the different stakeholders. The reliability of the results is monitored with the consistency measured and used as feed-back mechanism to ensure the quality of the judgements. Once agreed, the weights are used in PROMETHEE to calculate online a ranking of suspicious MV for each UAV. If two (or more) UAVs are assigned to the same MV, a mathematical programming formulation is employed to decide the assignment of the two UAVs by maximizing the sum of the PROMETHEE net flows. Finally, all missions can be viewed on a GIS for a post-analyis.

Two operators are needed to remotely control one UAV: one ground control pilot drives the UAV and the second one, the navigator, gives the route to the first one by looking at the MV and environmental data they receive. The latter operator could be replaced by the proposed system. Hence, the implementation enables a decrease in the number of operators by providing automated decision support to navigate the UAVs. This will lead to an increase in the probability of discovering illegal activites due to the more efficient use of time when identifying suspicious activities. Therefore, this system is a first significant step towards an autonomous UAV.

The hybrid set-up and use of MCDA techniques, namely AHP and PROMETHEE, facilitates the translation of surveillance expert knowledge into an advanced and automated decision support tool. It allows a high level of flexibility due to the combination of offline and online stages in the decision making. Hence, it allows for individual or combined amendments of the systems with regards to particular contextual preferences.

In order to further improve the system, future research work will investigate the UAVs success rate mission and use this information to feed-back to the system. This analysis can be used to fine tune the weights of the introduced environmental and mission criteria and depending on the context add or remove one or multiple critera. In this paper, we assume that all UAVs have the same capacity and can be used in any mission. Another avenue of future research is to take into account the capacities of each individual UAV (e.g. sensor capabilities, camera range, night vison, UAV autonomy, etc) to design their path mission.

Acknowledgements

This research has been partially funded by the European Commission Seventh Framework Programme with the SeaBILLA grant (241598).

6 References

Alemu, G. (2011). *GIS based and analytical network process based multi criteria decision aid for sustainable urban form selection of the Stockholm region.* Royal Institute of Technology (KTH), SE-100 44 STOCKHOLM, Sweden.

Aull–Hyde, R., & Davis, K. (2012). Military applications of the analytic hierarchy process. *International Journal of Multicriteria Decision Making, 2*, 267-281.

Aydogan, E. (2011). Performance measurement model for Turkish aviation firms using the rough-AHP and TOPSIS methods under fuzzy environment. *Expert Systems with Applications, 38*, 3992-3998.

Bigham, J., Cuthbert, L., Yang, X., Lu, N., & Ryan, D. (2004). Using intelligent agents for managing resources in military communications. *Computer Networks, 46*, 709-721.

Brans, J.-P., & Vincke, P. (1985). A preference ranking organisation method. *Management Science, 31*, 647-656.

Chen, S.-M. (1996). Evaluating weapon systems using fuzzy arithmetic operations. *Fuzzy Sets and Systems, 77*, 265-276.

Cheng, C.-H., & Lin, Y. (2002). Evaluating the best main battle tank using fuzzy decision theory with linguistic criteria evaluation. *European Journal of Operational Research, 142*, 174-186.

Cheng, C.-H., & Mon, D.-L. (1994). Evaluating weapon system by Analytical Hierarchy Process based on fuzzy scales. *Fuzzy Sets and Systems, 63*, 1-10.

Cheng, C.-H., Yang, K.-L., & Hwang, C.-L. (1999). Evaluating attack helicopters by AHP based on linguistic variable weight. *European Journal of Operational Research, 116*, 423-435.

Clark, B. (2015). Excel To KML - Display Excel files on Google Earth. In *Earth Point* (Vol. 2015).

Crary, M., Nozick, L., & Whitaker, L. (2002). Sizing the US destroyer fleet. *European Journal of Operational Research, 136*, 680-695.

Dagdeviren, M., Yavuz, S., & KilInç, N. (2009). Weapon selection using the AHP and TOPSIS methods under fuzzy environment. *Expert Systems with Applications, 36*, 8143-8151.

Feizizadeh, B., Jankowski, P., & Blaschke, T. (2013). A Spatially Explicit Approach for Sensitivity and Uncertainty Analysis of GIS-Multicriteria Landslide Susceptibility Mapping. 157-164.

Finan, J. S., & Hurley, W. J. (2002). The Analytic Hierarchy Process: Can Wash Criteria Be Ignored? . *Computers and Operations Research 29*, 1025-1030.

Gass, S. (1986). A Process for Determining Priorities and Weights for Large-Scale Linear Goal Programmes. *Journal of the Operational Research Society, 37*, 779-785.

Greiner, M., Fowler, J., Shunk, D., Carlyle, W., & McNutt, R. (2003). A hybrid approach using the analytic hierarchy process and integer programming to screen weapon systems projects. *Engineering Management, IEEE Transactions on, 50*, 192-203.

Haapalinna, I. (2003). How to allocate funds within the army. *European Journal of Operational Research, 144*, 224-233.

Hanscom, A., & Bedford, M. Unmanned Aircraft System (UAS) Service Demand 2015-2035.

Ishizaka, A., & Labib, A. (2011). Review of the main developments in the analytic hierarchy process. *Expert Systems with Applications, 38*, 14336-14345.

Ishizaka, A., & Nemery, P. (2013). *Multi-criteria Decision Analysis: Methods and Software*: Wiley.

Israeli, A., Mehrez, A., Bochen, D., & Hakim, D. (1998). Justification of global positioning systems purchase using the analytic hierarchical process—The case of the Israeli Defense Force. *Technovation, 18*, 409-424.

Joerin, F., Thériault, M., & Musy, A. (2001). Using GIS and outranking multicriteria analysis for land-use suitability assessment. *International Journal of ..., 15*, 153-174.

Kabak, M., Burmaoğlu, S., & Kazançoğlu, Y. (2012). A fuzzy hybrid MCDM approach for professional selection. *Expert Systems with Applications, 39*, 3516-3525.

Korkmaz, I., Gökçen, H., & Çetinyokus, T. (2008). An analytic hierarchy process and two-sided matching based decision support system for military personnel assignment. *Information Sciences, 178*, 2915-2927.

Lee, J., Kang, S., Rosenberger, J., & Kim, S. (2010). A hybrid approach of goal programming for weapon systems selection. *Computers & Industrial Engineering, 58*, 521-527.

Lee, Y., & Ahn, B. (1991). Static valuation of combat force potential by the analytic hierarchy process. *IEEE Transaction on Engineering Management, 38*, 237-244.

Lidouh, K. (2013). On The Motivation Behind MCDA and GIS Integration. *Int. J. of Multicriteria Decision Making, 3*, 101-113.

Lidouh, K., Smet, Y. D. E., & Zimányi, E. (2011). On the Integration of MCDA in GIS : Current Trends and Needed Advances. 1-21.

Lowe, D. R., Story, H. B., & Parsons, M. B. (2014). *US Army Unmanned Aircraft Systems (UAS)—a historical perspective to identifying and understanding stakeholder relationships.* Monterey, California: Naval Postgraduate School.

Malczewski, J. (1999). *GIS and multicriteria decision analysis*: John Wiley & Sons.

Merrick, J., & Harrald, J. (2007). Making decisions about safety in US ports and waterways. *Interfaces*, *37*, 240-252

Moon, C., Lee, J., & Lim, S. (2010). A performance appraisal and promotion ranking system based on fuzzy logic: An implementation case in military organizations. *Applied Soft Computing, 10*, 512-519.

Nasiri, H., Boloorani, A. D., Sabokbar, H. A. F., Jafari, H. R., Hamzeh, M., & Rafii, Y. (2013). Determining the most suitable areas for artificial groundwater recharge via an integrated PROMETHEE II-AHP method in GIS environment (case study: Garabaygan Basin, Iran). *Environmental monitoring and assessment, 185*, 707-718.

Partovi, F., & Epperly, J. (1999). A quality function deployment approach to task organization in peacekeeping force design. *Socio-Economic Planning Sciences, 33*, 131-149.

Retchless, T., Golden, B., & Wasil, E. (2007). Ranking US army generals of the 20th century: a group decision-making application of the analytic hierarchy process. *Interfaces*, *37*, 163-175.

Saaty, T. (1977). A scaling method for priorities in hierarchical structures. *Journal of Mathematical Psychology, 15*, 234-281.

Saaty, T. (1980). *The Analytic Hierarchy Process*. New York: McGraw-Hill.

Saaty, T. (1983). Conflict resolution and the Falkland Islands invasion. *Interfaces, 13*, 68-83.

Saaty, T., Vargas, L., & Barzilay, A. (1982). High-level decisions: a lesson from the Iran hostage rescue operation. *Decision Sciences*, *13*, 185-206.

Stannard, B., Zahir, S., & Rosenbloom, E. (2006). Application of analytic hierarchy process in multi-objective mixed integer programming for airlift capacity planning. *Asia-Pacific Journal of Operational Research, 23*, 61-76.

Teo, H. C. (2013). *Closing the gap between research and field applications for multi-UAV cooperative missions.* Monterey, California: Naval Postgraduate School.

Trainor, T., Parnell, G., Kwinn, B., Brence, J., Tollefson, E., & Downes, P. (2007). The US army uses decision analysis in designing Its US installation regions. *Interfaces, 37*, 253-264.

Veness, C. (2014). Movable Type Scripts. In *Calculate distance, bearing and more between Latitude/Longitude points* (Vol. 2014).

Wargo, C. A., Church, G. C., Glaneueski, J., & Strout, M. (2014). Unmanned Aircraft Systems (UAS) research and future analysis. In *Aerospace Conference, 2014 IEEE* (pp. 1-16).

Xu, E., & Zhang, H. (2013). Spatially-explicit sensitivity analysis for land suitability evaluation. *Applied Geography, 45*, 1-9.

7 Appendix - Calculation of suspiciousness criteria

The varying MV *parameters* related to the position of the MV:

- *Latitude (radians)*
- *Longitude (radians)*
- *Bearing (radians)*

These parameters are used to calculate the distance of the UAV to coast, island and UAV. However, the distance is not used as a row data in the criteria as the suspiciousness is not simply inversely linearly correlated to the distance. An Area Criteria Algorithm based on the sigmoid function (or Logistic function) is used (20).

$$\mathrm{CRIT_{Area}}(\mathrm{lat}_{MV_\kappa}, lon_{MV_\kappa}, \mathrm{HDG}) = \mathrm{CRIT_{Angle}}(\mathrm{lat_{AOI}}, \mathrm{lon_{AOI}}, \mathrm{HDG}) \times \mathrm{CRIT_{Range}}(\mathrm{lat}_{AOI}, \mathrm{lon_{AOI}}) \quad \text{(A.1)}$$

where, $(\mathrm{lat}_{MV_\kappa}, lon_{MV_\kappa})$: are the given geographical coordinates in radians (latitude, longitude) of the MV.

HDG: is the MV heading at given instance of time.

$(\mathrm{lat}_{AOI}, \mathrm{lon_{AOI}})$: is the fixed geographical coordinates in radians (latitude, longitude) at the centre of area of interest (AOI), i.e. island or coast

The angle criteria, $\mathrm{CRIT_{Angle}}$ is given by,

$$\mathrm{CRIT_{Angle}}(\mathrm{lat_{AOI}}, \mathrm{lon_{AOI}}, \mathrm{BRG}) = \frac{1 + e^{-\beta_a \times (1-\cos(\alpha))}}{1 + e^{(-\beta_a \times (\cos(\mathrm{BRNG}-\mathrm{HDG}) - \cos(\alpha))}} \quad \text{(A.2)}$$

where, α: is the limiting angle, asymptote of the sigmoid function.

β_a: is the steepness of the sigmoid for the angles/heading criteria

The denominator is used to normalize the function, whereas the bearing (BRNG) is given by:

$$\mathrm{BRNG} = \mathrm{atan2}(\sin(\mathrm{lon_{AOI}} - \mathrm{lon}_{MV_K}) * \cos(lat_{AOI}), \cos(lat_{MV}) * \sin(lat_{AOI}) - \sin(lat_{AOI}) * \cos(lon_{\mathrm{AOI}} - lon_{MV_K}) \quad \text{(A.3)}$$

The range criteria is given by,

$$\mathrm{CRIT_{Range}}(\mathrm{lat}_{AOI}, \mathrm{lon}_{AOI}) = \frac{1 + e^{-\beta_r}}{1 + e^{-\beta_r \times (\frac{\mathrm{dist}}{\mathrm{range}} - 1)}} \quad \text{(A.4)}$$

where, β_r: is the steepness of the sigmoid for the range criteria range: is a dimensional unit, which expresses the urgency of an MV as a distance from the centre of an AOI (asymptote of sigmoid function).

dist: the distance given by:

$$\mathrm{dist} = \mathrm{ER} \times \mathrm{c} \tag{A.5}$$

where, ER (Earth's Radius) = 6371 km

$$\mathrm{c} = 2 * \mathrm{atan2}\left(\sqrt{\mathrm{a}}, \sqrt{1-\mathrm{a}}\right) \quad (\mathit{Haversine\ formula}) \tag{A.6}$$

where,

$$\mathrm{a} = \sin^2((\mathrm{lat}_{AOI} - \mathrm{lat}_{MV_K})/2) + \cos(lat_{AOI}) * \cos\left(\mathrm{lat}_{MV_K}\right) * \sin^2((\mathrm{lon}_{AOI} - \mathrm{lon}_{MV_K})/2) \tag{A.7}$$

The suspiciousness of the MVs are calculated with PROMETHEE, based on the following criteria:

1. Dimension of MV

Given by satellite image

2. Change of Speed

a. Calculate distance d travelled in the time interval with (24), where, in equation (26) AOI is replaced by MV_k:

$$\mathrm{a} = \sin^2((\mathrm{lat}_{MV_K+t} - \mathrm{lat}_{MV_K})/2) + \cos\left(lat_{MV_K+t}\right) * \cos\left(\mathrm{lat}_{MV_K}\right) * \sin^2((\mathrm{lon}_{MV_K+t} - \mathrm{lon}_{MV_K})/2) \tag{A.8}$$

b. Calculate velocity, v using equation (28)

$$\mathrm{v} = d/t \tag{A.9}$$

where, t is the time interval

c. Calculate change in speed by taking the differences of speed at the beginning of the time interval and at the end of it.

3. Rendez-vous

a. Calculate the distance of the MV to the other MVs (24), where, in equation (26) AOI is replaced by MV_l

b. From a set of MVs, find the minimum distance of the most suspicious MV with its nearest MV.

4. **Distance to island**
    a. Calculate the distance of the MV from Lampedusa (A.5)
    b. Calculate Bearing (A.3)
    c. Calculate Critical Angle (A.2)
    d. Calculate Critical Range (A.4)
    e. Calculate Critical Area (A.1)

The constants used in our case study are, provided by the experts:

Lampedusa	
$\boldsymbol{\beta_\alpha}$	0.4
$\boldsymbol{\beta_r}$	0.01
$\boldsymbol{\alpha}$	30 ◦
range	200 km
latitude	35.515 ◦
longitude	12.580 ◦

5. **Distance to coast**
    a. Calculate the distance of the MV to the Coast of Sicily at Porto di Palma (A.5)
    b. Calculate Bearing (A.3)
    c. Calculate Critical Angle (A.2)
    d. Calculate Critical Range (A.4)
    e. Calculate Critical Area (A.1)

The constants used in our case study are, provided by the experts:

Pantelleria	
$\boldsymbol{\beta_\alpha}$	0.5
$\boldsymbol{\beta_r}$	0.1
$\boldsymbol{\alpha}$	30 ◦
range	250 km
latitude	37.167 ◦
longitude	13.717 ◦

6. **Distance UAV to MV**
    a. Calculate the location (coordinates) of the most suspicious MV (10, 11) in the next interval time
    b. Calculate the new heading a UAV is required to take for investigating the MV (14)

c. Calculate the distance (sea level) of the UAV defined by equation (17) to most suspicious MV, so that when this distance is < 10 km, the particular most suspicious MV is considered to be investigated and no further action on this MV is required any longer
d. Taking into account the actual flying height of the UAV, calculate the actual distance defined by the Pythagorean equation (18).

7. MAOC tagging

Is based on an external information received by the operator of the CGC, who decides to flag as highly suspicious a specific MVs.